Growth mechanisms of carbon nanotubes using controlled production in ultrahigh vacuum

H. Hövel,[a] M. Bödecker, B. Grimm, and C. Rettig
Experimentelle Physik I, University of Dortmund, D-44221 Dortmund, Germany

(Received 7 January 2002; accepted for publication 11 April 2002)

We present a method for the preparation of single walled carbon nanotubes (SWNTs) on a highly oriented pyrolytic graphite (HOPG) surface in ultrahigh vacuum (UHV), for which the preparation parameters for the production of metal clusters, fixed to nanometer sized pits on the surface, and the subsequent deposition of carbon can be controlled separately. Using cobalt as the cluster metal we carried out a comprehensive study concerning the influence of the substrate temperature (up to 900 °C) and the effective film thickness for the carbon evaporation. With scanning tunneling microscopy in UHV at room temperature and at $T=77$ K we observed single, separated SWNTs of about 50 nm length, which frequently were angled or branched and included junctions between sections of different tube diameters. With a statistical evaluation of tube diameters, tube lengths, and cluster heights, we obtained new insights into the growth mechanisms. An increase of tube diameters with increasing substrate temperature and a strong catalytic activity of cobalt clusters with sizes below 4 nm is in agreement with experimental results for the gas phase growth and recent calculations for several growth mechanisms. At $T=77$ K the atomic structures of the SWNT were imaged together with atomic resolution on the HOPG substrate. The presence of branched SWNTs and the observed alignment of the lattice structure of the SWNT and the HOPG both indicate that the tube growth in our case probably takes place at the moving end of the SWNT and not at the fixed clusters, different from recent experiments using chemical vapor deposition for nanotube growth on substrates. © *2002 American Institute of Physics.* [DOI: 10.1063/1.1483375]

I. INTRODUCTION

In the last few years activities in the field of carbon nanotubes have been rapidly growing, not only because of the principal interest in the properties of these new one dimensional nanostructures, but also because of several prospective areas of application, for example their special mechanical and electronic properties.[1] At present, open questions exist concerning especially the growth mechanisms,[2–5] but also the role of junctions between two nanotubes[6] or branched junctions of nanotubes.[7]

Single walled carbon nanotubes (SWNTs) are in most cases produced using transition metal clusters acting as catalytic centers.[8] Macroscopic amounts of SWNT material can be produced in gas phase growth using this technique.[5,9] In the gas phase the formation of metal clusters and the growth of nanotubes catalyzed by these clusters occur simultaneously. With a variation of the growth parameters and the analysis of the final result the separation of the different mechanisms is difficult. The growth of nanotubes on a surface was observed for the evaporation of carbon on surfaces, e.g., highly oriented pyrolytic graphite (HOPG).[10] For a controlled growth of SWNT in this case the use of transition metals as catalyst also seems to be important.[11,12]

To investigate the growth mechanisms it is beneficial to use a preparation method in which most of the different parameters can be controlled independently. The ideal experiment would be to separate the two steps, metal cluster growth and nanotube growth, with an independent control of both in temperature, evaporation rate etc., and to characterize the sample during the growth process.

In our experiments we aim for the concept of a ''complete surface-science experimental approach'' [13] for the measurement of the geometric and electronic properties of the nanotubes, i.e., the use of several independent methods like, e.g., scanning tunneling microscopy (STM) and spectroscopy, ultraviolet photoelectron spectroscopy (UPS), low energy electron diffraction, Auger electron spectroscopy, and electron energy loss spectroscopy in combination.[14] All these methods are very surface sensitive, and the use of ultrahigh vacuum (UHV) is a prerequisite for all of them. Ideally the sample system can be left in the same UHV apparatus to apply all techniques and hence minimize any problems related to the sample preparation. This excludes processes that use a rather high gas pressure[9] or chemical vapor deposition (CVD).[11]

The basis for the nanotube preparation as presented here is the method of ''controlled cluster growth on a nanostructured HOPG surface,'' [15] which was used to produce well defined silver clusters on a graphite surface for the measurement with STM and UPS[16] or for two photon photoemission.[17] In the following we will show that this technique can be used for the production of transition metal clusters, which then act as catalyst for the growth of SWNT. The main benefits of this method are that the parameters of the different preparation steps can be controlled independently, which gives new insights into the nanotube growth

[a]Author to whom correspondence should be addressed; electronic mail: hoevel@physik.uni-dortmund.de

mechanisms, and that it can be performed in UHV, which allows the use of surface sensitive techniques for their characterization as we mentioned above. Additionally we get well separated nanotubes, without the necessity of a subsequent decomposition of tube bundles.[18]

II. EXPERIMENT

First we produced nanopits 1 monolayer in depth and 5–10 nm in diameter on HOPG by sputtering and subsequent heating in an oxygen atmosphere. The details of this method are described in Refs. 15 and 19. For the development of the preparation method, which is presented here, a homogeneous size of the pits was not as important as it is for the use of nonlocal measurements as, e.g., photoemission spectroscopy.[16] So we could accept samples with a fraction of irregular shaped pits, which are formed in some cases, probably by the catalytic effect of contaminations during the oxidation process.[20] The nanostructured surface was then introduced into an UHV chamber for the following preparation steps. For the metal evaporation we used an electrically heated tungsten boat, and the carbon evaporation was achieved with a current of 100 A passing through a point contact between two carbon rods. The evaporation process was monitored with a quartz crystal balance. In this setup the chamber was not baked, but owing to a sufficiently high pumping speed we achieved a base pressure of 10^{-8} mbar. The maximal pressure occurring during the carbon evaporation was in the range of 10^{-6} mbar. The substrate was mounted on a sample holder which could be heated resistively, and the sample temperature was measured with a thermocouple.

Prior to the metal evaporation the HOPG with the nanopits was heated at 600 °C for 1 h, which cleans the surface, as we checked in previous experiments with UPS.[16] Then the metal evaporation was performed with the substrate at room temperature. If not mentioned otherwise we used a metal coverage corresponding to an effective metal film thickness of 0.2 nm, which resulted in a mean cluster height of about 4 nm similar to the silver cluster sample of Ref. 15. For a few samples we checked by STM that this results in the growth of transition metal clusters fixed in the nanopits, but we could image the clusters after the carbon evaporation as well, so in most cases the STM measurements were performed for the complete sample with clusters and nanotubes.

Concerning the carbon coverage we varied the substrate temperature during evaporation and the effective film thickness as measured with the quartz crystal balance. In this way we produced more than ten different samples in order to study and optimize the nanotube growth mechanism, some of which are discussed in detail below. To avoid an overheating of the evaporation setup, the carbon had to be evaporated in intervals of about 1 s with short breaks inbetween. Waiting for a thermal equilibrium of the quartz crystal, the effective film thickness was checked every 10 s total evaporation time, with an increase of about 0.3 nm in this interval.

In the experiments described here we imaged the samples in a separated UHV–STM at room temperature or at $T=77$ K. After the metal and the carbon evaporation were performed in UHV the final topology of the sample is not influenced by this transfer. Especially for the measurement at $T=77$ K we heated the sample to 300 °C in UHV before STM imaging in order to remove adsorbed water. We checked that this did not change the sample topology. In future experiments we will combine the preparation and the analysis in the same UHV apparatus in order to use the concept of a complete surface-science experimental approach, as it was described above.

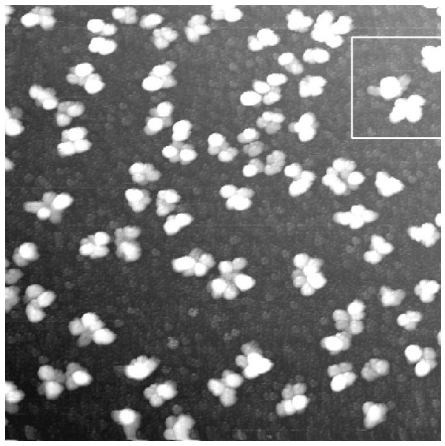

FIG. 1. STM image (300×300 nm^2, room temperature) of a HOPG surface with preformed Co clusters and 0.2 nm carbon coverage evaporated at room temperature. Most of the carbon covers the sample as an amorphous film, some elongated structures attached to the Co clusters (e.g., in the marked area) may be interpreted as the onset of a tube growth.

III. RESULTS

We started our experiments using Fe as cluster material. For the substrate temperature we tried room temperature and 575 °C. In this experiments we did not observe structures which could be assigned to a tube growth. The carbon formed amorphous structures on the clusters and, with the substrate at room temperature, inbetween them. Since for similar conditions we did observe tube growth in the case of Co clusters, which we used in the following experiments, we suspect that the catalytic effect of Co is stronger than for Fe under the experimental conditions used here. But more experiments focusing on the different cluster materials with the other parameters kept identical have to be performed before a final conclusion can be given.

For Co as cluster material we carried out a comprehensive study concerning the influence of the substrate temperature and the effective film thickness for the carbon evaporation. We discuss a few of the samples in more detail to analyze the influence of these parameters on the nanotube growth.

With the substrate kept at room temperature an effective film thickness of 0.2 nm carbon was sufficient to observe a significant amount of carbon induced structures additional to the Co clusters, which shows that the sticking coefficient has to be close to 1. Most of the carbon formed amorphous structures covering all the surface area between the clusters, with no clean HOPG areas left, as shown in Fig. 1. In this STM image the carbon is visible as a granular structure between

the clusters, as compared to the totally flat clean HOPG areas shown below, e.g., in Fig. 2. This suggests little diffusion of the carbon atoms so that they remain the place where they hit the surface. Some carbon is also attached to the Co clusters, which are clearly distinguishable from the amorphous carbon film with their mean height of 4 nm. In most cases the carbon forms small humps attached to the clusters. But at a few of the Co clusters, we observed elongated additional structures with a height of about 1.5 nm, which may be interpreted as the onset of a tube growth. Some of these features are visible in the marked area in Fig. 1.

In Fig. 2 we show a STM image with the substrate covered with 0.2 nm carbon at a temperature of 600 °C. Between the Co clusters the clean HOPG surface shows up. This indicates an increased diffusion of the carbon atoms. Long linear structures with a height of about 1 nm as marked with an arrow in Fig. 2 prove the growth of SWNT. The special tube structure on this image looks like a closed ring. Closed rings were recently observed for chemically reacted SWNT.[21] But this special shape here is accidental because we also observed linear tubes on this sample, looking like those shown below in Fig. 4. The total amount of carbon on the surface is much smaller than for the same carbon evaporation with the substrate at room temperature. This shows that the sticking coefficient is now significantly smaller than 1. We imaged 23 different tube structures on this sample, so we can give values for the mean tube diameter, measured as the height with respect to the substrate surface. The height of the tubes is not affected by a convolution with the shape of the tip, however it may be influenced by a change in the tip–sample distance. Since we use a graphite substrate the tip–sample distance is similar for the substrate and the nanotube and the height measures the tube diameter more exactly than the lateral width combined with a deconvolution of the tip shape. Additionally we evaluated the number of tubes per area, and the total tube length per area. These numbers are given in Table I together with the corresponding data for the following samples. We show histograms for the tube diameters in Fig. 3.

With 900 °C substrate temperature we produced three samples with an evaporated carbon coverage of 0.25, 3, and 15 nm, respectively. For 0.25 nm only a few short tubes and one longer tube were found on a large number of STM images, which was not enough to give average tube parameters. This shows that the sticking coefficient is further decreased with respect to 600 °C substrate temperature. With an increased carbon coverage of 3 nm we observe a large number of carbon nanotubes, all attached to Co clusters. A typical

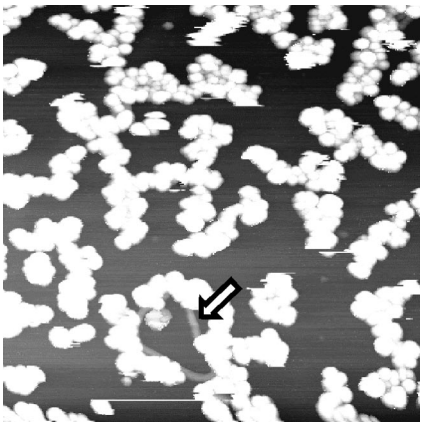

FIG. 2. STM image (300×300 nm^2, room temperature) of a HOPG surface with preformed Co clusters and 0.2 nm carbon coverage evaporated at $T=600$ °C. Some SWNT show up as long linear structures with a height of about 1 nm (marked with arrow).

image is shown in Fig. 4. The tube structures show junctions of tubes of different diameter (see mark A) and branched tube junctions (see mark B). They may be formed because the carbon was evaporated intermittently. For such tubes the mean tube diameter was calculated by averaging over several line profiles measured for the different sections of the tubes. In addition to the nanotubes one can see carbon islands, one carbon monolayer, i.e., 0.35 nm, in height, which grow attached to the clusters structures (see mark C).

In Figs. 5(a)–5(c) we show three of the observed branched junctions in more detail. In particular, the junction in Fig. 5(c) seems to be very uniform. This, together with the angles very close to 120° between the three branches, suggests a regular geometric structure similar to the ones calculated in Ref. 22. In these calculations three equal tubes were connected, but in our experimental result the tubes are different. The long tube has a height of 1.3 nm, while the two short tubes have heights of 0.7 and 0.8 nm. The branched junctions in Figs. 5(a) and 5(b) seem to include more defects. But nevertheless preferentially angles close to 90° or 120° occur, which indicate structures with some regularity.

In Fig. 6 we present detailed images of a SWNT on this sample, which were measured at $T=77$ K. We found the use of low temperature STM in UHV advantageous to a simultaneous atomic resolution on the HOPG substrate and the nanotube. In Fig. 6(a) the overview shows a tube structure of about 50 nm length with a junction between a longer tube of 1.7 nm height, which is slightly angled and a shorter tube of 1.3 nm in height. Figure 6(b) displays a section of a

TABLE I. Results of the statistical evaluation for the carbon nanotubes produced on three samples with different parameters for the sample temperature and the effective carbon coverage. Given are the mean tube diameter, measured as the height with respect to the substrate surface, the number of tubes per area, and the total tube length per area, extracted from several STM images taken on each of these three samples.

Sample temperature (°C)	Effective carbon film thickness (nm)	Mean tube diameter (nm)	Number of tubes per area (μm^{-2})	Total tube length per area (μm^{-1})
600	0.2	1.1	50 ± 10	0.8 ± 0.2
900	3	1.3	220 ± 30	3.5 ± 0.5
900	15	2.4	260 ± 30	4.6 ± 0.5

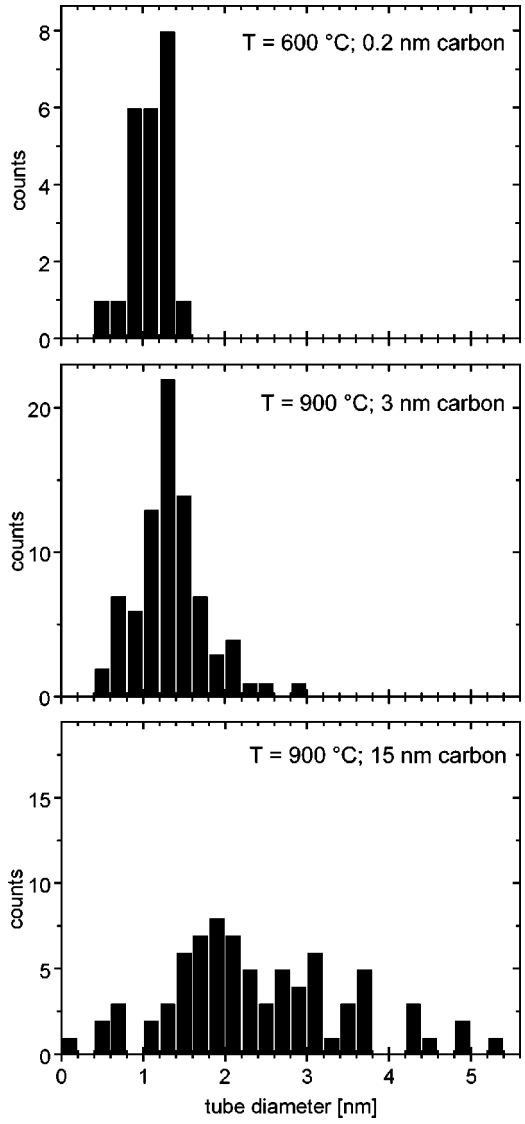

FIG. 3. Histograms of tube diameters, measured as the height in the STM images, for three samples with different sets of growth parameters. The sample temperature and the effective film thickness for the carbon evaporation is given for each histogram.

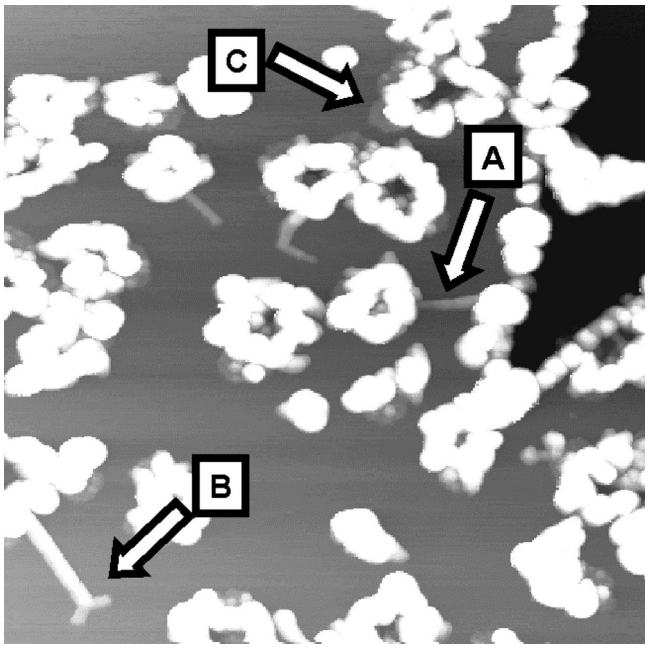

FIG. 4. STM image (300×300 nm^2, room temperature) of a HOPG surface with preformed Co clusters and 3 nm carbon coverage evaporated at $T=900$ °C. Visible are several SWNT attached to the clusters. Some include junctions of tubes with different diameter (A) or branched junctions (B). Additionally carbon islands have grown, 1 monolayer in height (C).

tube with atomic resolution. We get a reasonably good description of the atomic tube structure, if we construct a graphite lattice which fits the simultaneously imaged graphite substrate and expand it perpendicular to the tube axis, which is a known effect in the STM imaging of nanotubes.[23] This indicates an orientation of the tubes given by an alignment of the tube graphene structure with the lattice of the graphite substrate. Such an alignment was also found for all other tubes imaged with atomic resolution on this sample. We will discuss this in more detail in a separate paper using a quantitative evaluation of the lattice alignment. The junction visible in Fig. 6(a) is shown in detail in Fig. 6(c) with atomic resolution. At the junction between the different tube sections we observe extra hillocks in the STM image. This can be observed even better in the three-dimensional (3D) display of another junction (Fig. 7). The hillocks can be explained with an electronic effect in calculated STM images due to the pentagonal and heptagonal defects which are incorporated in these junctions.[23]

In order to clarify which cluster sizes have the strongest catalytic effect for the nanotube growth, we evaluated the cluster heights for the sample covered with 3 nm effective carbon film thickness at 900 °C, distinguishing between clusters which are connected to a tube and those which are not. The resulting histograms for all clusters and only these clusters which are connected to a tube are shown in Fig. 8. One clearly observes that clusters with heights below 4 nm show a stronger catalytic effect for the nanotube growth. This is in agreement with calculations, showing that high local curva-

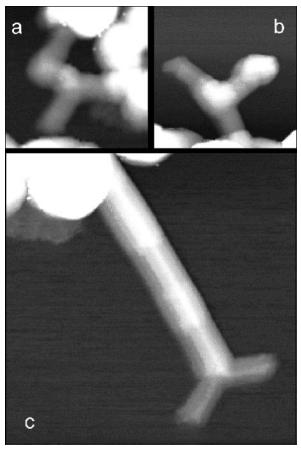

FIG. 5. Detailed images of three branched junctions on the sample as shown in Fig. 4. STM at room temperature, image sizes: (a), (b) 40×40 nm^2, and (c) 60×60 nm^2.

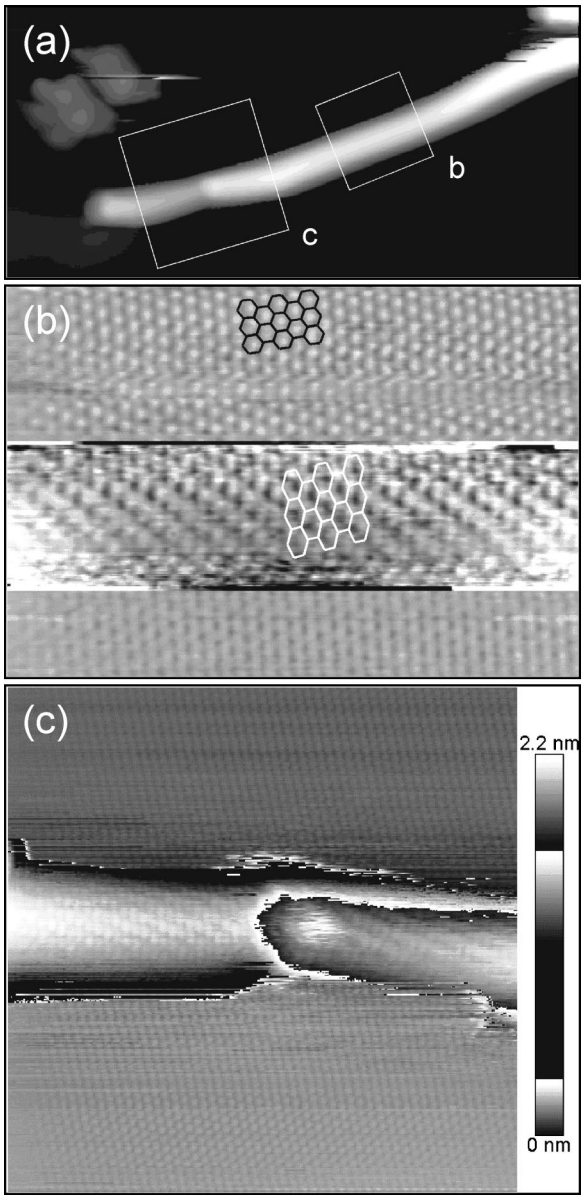

FIG. 6. STM images of a SWNT taken at $T=77$ K on the sample as shown in Fig. 4: (a) overview (63×30 nm^2) in the marked areas the following atomically resolved images were taken. (b) Tube imaged with atomic resolution (10×7 nm^2). The lattice fitted to the HOPG substrate (black) also fits to the tube lattice if it is expanded perpendicular to the tube axis (white). (c) Junction between two SWNTs of different diameter imaged with atomic resolution (15×15 nm^2). In the two lower images a background correction or a stepwise color table was used, respectively, in order to stretch the color scaling available for the atomic structure.

tures on a metal surface with radii of a few nanometers are needed for the nucleation of SWNT.[24]

A carbon coverage of 15 nm at 900 °C is shown in the STM image of Fig. 9. As an additional change we decreased the Co coverage to 0.1 nm effective film thickness in this case, which should give slightly smaller cluster sizes. The reason for this change was that clusters with a height below 4 nm were more effective for a catalysis of nanotube growth, as discussed above. The parameters in Table I show that the tube length per area has increased only moderately, and larger tube diameters are observed. Additionally one can see more carbon islands, with a height of up to 2 monolayers and

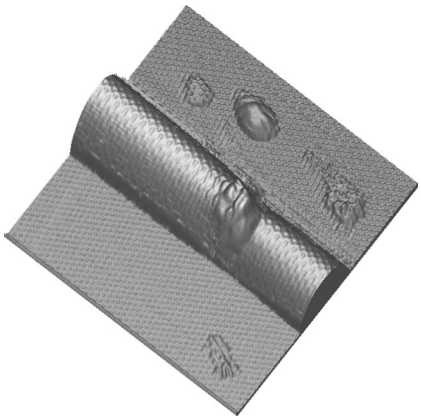

FIG. 7. 3D display of a junction between two SWNT of different diameter taken at $T=77$ K on the sample as shown in Fig. 4 (14×14 nm^2) for a different tube than the one shown in Fig. 6(c).

also a significant carbon coverage on the clusters, which show heights up to 13 nm.

IV. DISCUSSION

With the STM images shown and the statistical evaluation of many more images of these samples given in Table I and Fig. 3 several conclusions can be drawn concerning the nanotube growth mechanisms.

We observe that the nanotubes are always connected to Co clusters. This shows that these clusters act as catalytic centers. In particular, clusters with heights below 4 nm show a strong catalytic effect. Two growth models would be com-

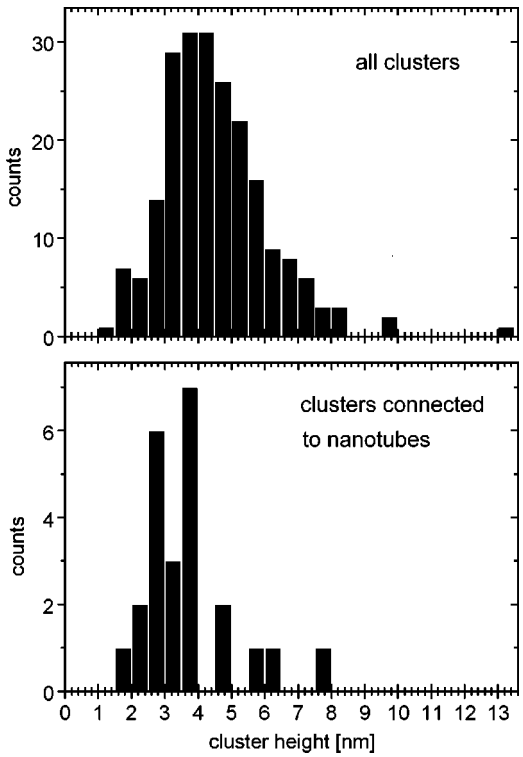

FIG. 8. Histogram of the cluster heights on the sample as shown in Fig. 4, counted separately for all clusters and only for those connected to a nanotube.

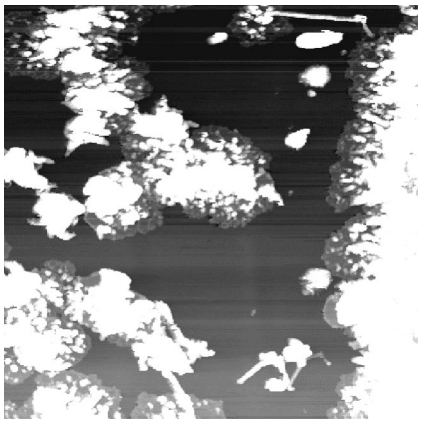

FIG. 9. STM image (300×300 nm^2, room temperature) of a HOPG surface with preformed Co clusters and 15 nm carbon coverage evaporated at $T=900$ °C. Visible are several NT and carbon islands 1 and 2 monolayer in height.

patible with our results. First, the tube growth may proceed at the moving end of the tube after it has started by the catalytic effect of the cluster, possibly under the influence of a few cobalt atoms moving with the open end.[25] Second, the carbon atoms may be incorporated into the tube at the cluster.[2,24] Currently most experiments for nanotube growth on substrates can be explained in the frame of such a ''root growth'' at clusters of the same size or larger than the nanotube diameters. But in recent experiments investigating the mechanisms for the gas phase growth of SWNT,[5] at least the start of the nanotube growth happens before large metal clusters are formed. Since in our experiments the clusters are fixed to the nanopits prior to the carbon coverage, the tubes have to move along the surface during the growth process, if we assume that the carbon atoms are incorporated at the clusters. The interaction between a SWNT and the HOPG surface is similar to that between two graphite planes which is weak and van der Waals in origin. With this a binding energy of about 2 eV per nm tube length was calculated for SWNT of similar diameter on a graphite surface.[26,27] However this binding energy corresponds to the perpendicular force between the tube and the surface, and the lateral forces may be much smaller. The lateral forces are indeed extremely small if the tube lattice is out of registry with the graphite lattice, but energy barriers of about 0.03 eV per nm tube length occur for a sliding motion if the nanotube and the graphite lattice are in registry, as was shown experimentally[28] and in calculations.[27] In our experiments we observed an orientation of the tube lattice in registry with the HOPG [cf. Fig. 6(b)], which renders a sliding motion of the tubes during the growth process unlikely for tube lengths larger than 10 nm. Therefore the tube growth in our case probably proceeds at the moving end, different from the growth observed, e.g., using CVD of carbon.[11] A growth at the moving end is also indicated by the branched junctions as in Fig. 5. In the case of a growth at the fixed clusters one has to assume two previously separated nanotubes which join in the growth process. For a growth at the moving end the formation of branched junctions is more naturally explained by the incorporation of defects during growth.

The observed SWNT growth parallel to the surface can be explained with the transport of carbon atoms due mainly to surface diffusion. The low sticking coefficient at high temperature suggests growth by a two-dimensional nucleation of mobile adsorbed carbon atoms, similar to the case of metal atoms on HOPG at room temperature.[29] This is supported by the observation of monolayer–carbon islands attached to the clusters with large uncovered areas inbetween, e.g., in Fig. 9, additional to the SWNT.

The data in Table I and Fig. 3 indicate that with increasing temperature the fraction of larger tube diameters increased, while the lower limit of the tube diameters remained nearly constant. This is in agreement with the experimental data obtained for gas phase growth of SWNT[3] and theoretical models, which explain this observation with the size dependence of the energy needed to open a double-layered graphitic patch[4] or to detach precipitated graphene sheets from the surface of the metal particle.[2]

For all three samples the mean tube length is approximately 16 nm. We observed a large number of short tubes but also tubes with a length of 60–70 nm on every sample. A comparison of the two samples grown at 900 °C shows that with increasing effective carbon film thickness the number of tubes per area has remained constant within the error bars. Also the total tube length per area is not significantly larger. Instead the tube diameters have increased strongly. For the sample with 15 nm effective film thickness some tubes have diameters which would be compatible also with multiwalled nanotubes. This may indicate that there is only a certain amount of catalytically active positions and the additional carbon is built into the existing tubes, also possibly forming multiwalled nanotubes, and also into a larger number of carbon islands.

Finally, we compare our results with the production of SWNT with CVD. They mainly differ in the kind of carbon supply for the nanotube growth. With our method the carbon atoms diffuse laterally on the surface before they are incorporated, e.g., at the moving end of the SWNT. For the growth of SWNT using CVD the carbon supply is given by carbon atoms dissolving in the metal nanoparticles. After saturation the carbon precipitates to form solid carbon tubes, which also often results in growth perpendicular to the surface and can lead to the production of long, defect free SWNT.[11] In contrast, within our production method, the condensation of carbon atoms, which approach by surface diffusion naturally leads to a growth parallel to the surface but it may also more easily cause the introduction of defects during growth. Less defects might be expected for sample temperatures higher than 900 °C, but this is limited by the already very low sticking coefficient at this temperature.

V. CONCLUSION

We have presented a method for the controlled growth of single walled carbon nanotubes on a graphite surface in UHV. The independent control of the parameters for the cluster growth and the carbon evaporation gave new insights into the growth mechanisms.

We observed a catalytic effect of cobalt clusters for the nanotube growth, which is significantly stronger for cluster sizes below 4 nm. Linear, angled, and branched carbon nanotubes connected to the cobalt clusters were imaged with STM in UHV. The fraction of larger tube diameters increases with increasing substrate temperature, which is in agreement with experimental results for gas phase growth and with recent calculations for several growth mechanisms.

The detailed mechanisms of nanotube growth in general are still a topic of current research. The experimental results indicate that for our production method the tube growth takes place at the moving end of the tubes, different from recent experiments using CVD for nanotube growth on substrates. This is probably caused by the supply of carbon atoms, which in our case approach by surface diffusion. The clusters in the nanopits are fixed to the substrate, and a sliding motion of the tubes during growth is unlikely if we consider the frequent occurrence of branched junctions and the observed alignment between the atomic tube structure and the graphite substrate, which indicates a tube–surface interaction.

ACKNOWLEDGMENT

The authors would like to acknowledge support by the Deutsche Forschungsgemeinschaft (Ho-1597/3-3).

[1] Phys. World **13**, 29 (2000); H. W. Ch. Postma, T. Teepen, Z. Yao, M. Grifoni, and C. Dekker, Science **293**, 76 (2001).
[2] H. Kanzow and A. Ding, Phys. Rev. B **60**, 11180 (1999); H. Kanzow, C. Lenski, and A. Ding, *ibid.* **63**, 125402 (2001).
[3] S. Bandow, S. Asaka, Y. Saito, A. M. Rao, L. Grigorian, E. Richter, and P. C. Eklund, Phys. Rev. Lett. **80**, 3779 (1998).
[4] P. Zhang and V. H. Crespi, Phys. Rev. Lett. **83**, 1791 (1999).
[5] C. D. Scott, S. Arepalli, P. Nikolaev, and R. E. Smalley, Appl. Phys. A: Mater. Sci. Process. **72**, 573 (2001).
[6] J. Han, M. P. Anantram, R. L. Jaffe, J. Kong, and H. Dai, Phys. Rev. B **57**, 14983 (1998); Z. Yao, H. W. Ch. Postma, L. Balents, and C. Dekker, Nature (London) **402**, 273 (1999).
[7] J. Li, C. Papadopoulos, and J. Xu, Nature (London) **402**, 254 (1999); B. C. Satishkumar, P. J. Thomas, A. Govindaraj, and C. N. R. Rao, Appl. Phys. Lett. **77**, 2530 (2000); P. Nagy, R. Ehlich, L. P. Biro, and J. Gyulai, Appl. Phys. A: Mater. Sci. Process. **70**, 481 (2000); M. Ouyang, J.-L. Huang, C. L. Cheung, and C. M. Lieber, Science **291**, 97 (2001); C. Papadopoulos, A. Ratikin, J. Li, A. S. Vedeneev, and J. M. Xu, Phys. Rev. Lett. **85**, 3476 (2000).
[8] D. S. Bethune, C. H. Kiang, M. S. de Vries, G. Gorman, R. Savoy, J. Vazques, and R. Beyers, Nature (London) **363**, 605 (1993).
[9] A. G. Rinzler *et al.*, Appl. Phys. A: Mater. Sci. Process. **67**, 29 (1998).
[10] M. Ge and K. Sattler, Science **260**, 515 (1993).
[11] J. Kong, H. T. Soh, A. M. Cassell, C. F. Quate, and H. Dai, Nature (London) **395**, 878 (1998); J. Kong, A. M. Cassell, and H. Dai, Chem. Phys. Lett. **292**, 567 (1998).
[12] W. Z. Li, S. S. Xie, L. X. Qian, B. H. Chang, B. S. Zou, W. Y. Zhou, R. A. Zhao, and G. Wang, Science **274**, 1701 (1996); R. R. Schlittler, J. W. Seo, J. K. Gimzewski, C. Durkan, M. S. M. Saifullah, and M. E. Welland, *ibid.* **292**, 1136 (2001).
[13] H. Hövel, L. S. O. Johansson, and B. Reihl, in: *Metal Clusters at Surfaces*, edited by K. H. Meiwes-Broer, Springer Series in Cluster Physics (Springer, New York, 2000), pp. 37–65.
[14] H. Hövel, T. Becker, D. Funnemann, B. Grimm, C. Quitmann, and B. Reihl, J. Electron Spectrosc. Relat. Phenom. **88–91**, 1015 (1998).
[15] H. Hövel, Th. Becker, A. Bettac, B. Reihl, M. Tschudy, and E. J. Williams, J. Appl. Phys. **81**, 154 (1997).
[16] H. Hövel, B. Grimm, M. Pollmann, and B. Reihl, Phys. Rev. Lett. **81**, 4608 (1998).
[17] M. Merschdorf, W. Pfeiffer, A. Thon, S. Voll, and G. Gerber, Appl. Phys. A: Mater. Sci. Process. **71**, 547 (2000).
[18] J. Liu *et al.*, Science **280**, 1253 (1998).
[19] H. Hövel, Appl. Phys. A: Mater. Sci. Process. **72**, 295 (2001).
[20] H. Chang and A. J. Bard, J. Am. Chem. Soc. **113**, 5588 (1991).
[21] M. Sano, A. Kamino, J. Okamura, and S. Shinkai, Science **293**, 1299 (2001).
[22] G. E. Scuseria, Chem. Phys. Lett. **195**, 534 (1992); G. Treboux, P. Lapstun, Z. Wu, and K. Slverbrook, J. Phys. Chem. B **103**, 8671 (1999).
[23] V. Meunier and Ph. Lambin, Phys. Rev. Lett. **81**, 5588 (1998).
[24] A. Maiti, C. J. Brabec, and J. Bernholc, Phys. Rev. B **55**, 6097 (1997).
[25] A. Thess *et al.*, Science **273**, 483 (1996); Y. H. Lee, S. G. Kim, and D. Tomanek, Phys. Rev. Lett. **78**, 2393 (1997).
[26] T. Hertel, R. E. Walkup, and P. Avouris, Phys. Rev. B **58**, 13870 (1998).
[27] A. Buldum and J. P. Lu, Phys. Rev. Lett. **83**, 5050 (1999).
[28] M. R. Falvo, J. Steele, R. M. Taylor II, and R. Superfine, Phys. Rev. B **62**, 10 665 (2000); H. Yanagi, E. Sawada, A. Manivannan, and L. A. Nagahara, Appl. Phys. Lett. **78**, 1355 (2001); K. Miura, M. Ishikawa, R. Kitanishi, M. Yoshimura, K. Ueda, Y. Tatsumi, and N. Minami, *ibid.* **78**, 832 (2001).
[29] J. R. Arthur and A. Y. Cho, Surf. Sci. **36**, 641 (1973).